



A block zero-padding method based on DCFT for L1 parameter estimations in weak signal and high dynamic environments*

Chao WU[†], Lu-ping XU, Hua ZHANG, Wen-bo ZHAO

(School of Aerospace Science and Technology, Xidian University, Xi'an 710126, China)

[†]E-mail: wuchaoid@126.com

Received Feb. 13, 2015; Revision accepted Apr. 13, 2015; Crosschecked July 24, 2015

Abstract: Weak L1 signal acquisition in a high dynamic environment primarily faces a challenge: the integration peak is negatively influenced by the possible bit sign reversal every 20 ms and the frequency error. The block accumulating semi-coherent integration of correlations (BASIC) is a state-of-the-art method, but calculating the inter-block conjugate products restricts BASIC in a low signal-to-noise ratio (SNR) acquisition. We propose a block zero-padding method based on a discrete chirp-Fourier transform (DCFT) for parameter estimations in weak signal and high dynamic environments. Compared with the conventional receiver architecture that uses closed-loop acquisition and tracking, it is more suitable for open-loop acquisition. The proposed method combines DCFT and block zero-padding. In this way, the post-correlation signal is coherently post-integrated with the bit sequence stripped off, and the high dynamic parameters are precisely estimated using the threshold set based on a false alarm probability. In addition, the detection performance of the proposed method is analyzed. Simulation results show that compared with the BASIC method, the proposed method can precisely detect the high dynamic parameters in lower SNR when the length of the received signal is fixed.

Key words: Threshold detection, Discrete chirp-Fourier transform, Block zero-padding, High dynamic, Weak L1 signal acquisition
doi:10.1631/FITEE.1500058 **Document code:** A **CLC number:** TN961

1 Introduction

The Global Positioning System (GPS) signal is modulated by the direct sequence spread spectrum technique. Every satellite is transmitting a particular pseudorandom noise (PRN) code. The L1 signal is an important component of GPS (Huang *et al.*, 2013).

When the signal transmission environments are not ideal, such as interior, forest, and urban environments, acquiring the signal would cause a serious energy decline. To solve this problem, a general approach is to increase the integration time (Yang and Han, 2001) over the PRN code periods, which leads to a high integration peak and increases the detection probability (Geiger *et al.*, 2012; Geiger and Vogel, 2013). However, weak L1 acquisition in the high dynamic environment faces the following challenge: the integration peak is negatively influenced by the possible bit sign reversal every 20 ms and the frequency error.

To reduce the influence of the frequency error on the integration peak, Spangenberg *et al.* (2000), Shanmugam *et al.* (2007), and Dai *et al.* (2010) performed the Doppler compensation on the correlation based on the chirp signal or signal block. The detection probability is improved when the high

* Project supported by the National Natural Science Foundation of China (Nos. 61172138 and 61401340), the Natural Science Basic Research Plan in Shaanxi Province of China (No. 2013JQ8040), the Research Fund for the Doctoral Program of Higher Education of China (No. 20130203120004), the Open Research Fund of the Academy of Satellite Application (No. 2014_CXJJ-DH_12), the Xi'an Science and Technology Plan (No. CXY1350 (4)), the Fundamental Research Funds for the Central Universities (Nos. 201413B, 201412B, and JB141303), and the Open Fund of Key Laboratory of Precision Navigation and Timing Technology, National Time Service Center, CAS (Nos. 2014PNTT01, 2014PNTT07, and 2014PNTT08)

ORCID: Chao WU, <http://orcid.org/0000-0001-7769-6155>

© Zhejiang University and Springer-Verlag Berlin Heidelberg 2015

precision frequency estimation is obtained. The high precision frequency estimation has been extensively studied in Kay (1989), Fu and Kam (2007), and Belega and Dallet (2008). However, due to the acceleration and instability of the local clock in high dynamic acquisition (Su and Wu, 2000), the phase of the complex baseband signal without noise (or frequency error) is nonlinear. Therefore, the block accumulating semi-coherent integration of correlations (BASIC) method (Yang *et al.*, 2008) has been proposed. This method converts the nonlinear problem into a linear one. This is achieved by calculating the inter-block conjugate products. Moreover, to reduce the influence of bit sign reversal on the integration peak, block zero-padding is used. This process consists of two steps. The first step is to divide the inter-block conjugate products into a few blocks. The second step is pre- and post-zero-padding each block for maintaining its timing order in the original sequence. In this way, the negative effects of the bit sign sequence (BSS) on the integration peak have been removed, and each block can be coherently integrated by the following processes when bit synchronization occurs. The method uses fast Fourier transform (FFT) to estimate the chirping rate, which is also known as the block zero-padding method based on FFT in this paper. However, it brings new noise terms, which is not good for acquisition under the low signal-to-noise ratio (SNR). Fan *et al.* (2013) proposed the frequency estimation method based on discrete chirp-Fourier transform (DCFT). This method can improve the probability of detecting the integration peak without calculating the inter-block conjugate products. Moreover, DCFT can estimate the Doppler shift and Doppler rate of an L5 signal at the same time. However, it cannot directly be applied in an L1 signal acquisition owing to the influence of the possible bit sign reversal every 20 ms on the integration peak.

To avoid the influence of the possible bit sign reversal every 20 ms on the integration peak, the differential coherence based bit synchronization algorithm has been proposed for high dynamic and weak GPS signals (Li *et al.*, 2011; Li and Guo, 2013). First, the coherent integration values are processed by the differential coherence. Then the differential coherence values are accumulated according to the 20

navigation bit sign boundary candidates as the decision variable. Finally, to achieve bit synchronization, the navigation bit sign boundary candidate corresponding to the minimum or maximum of these decision variables is determined as the navigation bit sign boundary position. Although these methods find the navigation bit sign boundary position, how to obtain the bit sign is not discussed.

In this paper we propose a novel acquisition method for parameter estimations in weak signal and high dynamic environments. Due to the influence of bit sign reversal and the frequency error on the integration peak, the post-correlation signal in the high dynamic environment cannot be directly used for integration. So, the signal is processed by the block zero-padding method based on DCFT. First, the post-correlation signal is divided into a few blocks by block zero-padding. Then each block is processed by DCFT. In this way, the post-correlation signal can be coherently post-integrated, and the influence of BSS on the integration peak can be eliminated. Finally, the high dynamic parameters (including BSS, chirping rate, and initial frequency) are estimated based on the integration peak obtained using the threshold set based on a false alarm probability, and the theoretical performance of the proposed method can be analyzed. The simulation results show that compared with BASIC, the proposed method can estimate the high dynamic parameters in a lower SNR.

2 High dynamic L1 signal model

Based on the analysis in Yang *et al.* (2008), the baseband L1 signal of a specific satellite vehicle (SV) through the 1 ms correlation process can be written as

$$\begin{aligned} x_n &= b_n A \exp\{j[2\pi(f_0 n T_s + \alpha n^2 T_s^2) + \phi_0]\} + w_n \\ &= s_n + w_n, \end{aligned} \quad (1)$$

where w_n is the post-correlation noise, x_n the post-correlation signal with noise, s_n the post-correlation signal without noise, $b_n = \pm 1$ the unknown data bit or bit sign, n the sampling point index, A the amplitude of the 1 ms correlation, T_s the sampling interval of the post-correlation, f_0 the initial frequency, α the chirping rate, and $f_0 n T_s + \alpha n^2 T_s^2$ the frequency error.

3 Block zero-padding method based on DCFT for parameter estimations in weak signal and high dynamic environments

In this section, we analyze the two conventional methods, i.e., BASIC and DCFT. Based on the analysis, we combine the two methods and propose a novel method for parameter estimations in weak signal and high dynamic environments.

3.1 Conventional methods

To process the post-correlation signal and obtain the initial frequency chirping rate and bit sign, the block diagram of BASIC has been proposed. This is the block zero-padding method based on FFT. However, constructing the inter-block conjugate products limits BASIC in obtaining the high dynamic parameters when SNR is low. Moreover, estimating the high dynamic parameters by detecting the integration peak leads to incorrect estimations of the high dynamic parameters when the signal is absent or misaligned with the local code. The BASIC diagram can be drawn as Fig. 1 (Yang *et al.*, 2008).

As can be seen from Eq. (1), the phase of s_n changes nonlinearly with n and the complex post-correlation signal is affected by the frequency error and bit sign. The BASIC method constructs the inter-block conjugate products:

$$\begin{aligned} z_{ki} &= x_{(k+1)M+i} x_{kM+i}^* \\ &= s_{(k+1)M+i} s_{kM+i}^* + w_{kM+i}^* s_{(k+1)M+i} \\ &\quad + w_{(k+1)M+i} s_{kM+i}^* + w_{kM+i} w_{(k+1)M+i}^* \\ &= b_{k+1} b_k A^2 \exp\left\{2\pi j \left[f_0 \gamma + \alpha(2k+1)\gamma^2 + 2\alpha\gamma T_s i \right]\right\} + W \\ &= b_{k+1} b_k A^2 \exp(\Psi(k, i)) + W, \end{aligned} \quad (2)$$

where * represents the conjugate operation, $\gamma = MT_s$, i represents the i th sampling point per block, M is the number of sampling points per block, and $k=1, 2, \dots, K$ (K is the number of blocks or bit periods, i.e., 20 chip periods). As can be seen from Eq. (2), phase $\Psi(k, i)$ changes linearly with variables i and k , and the estimate for α is regarded as a linear problem. However, it brings new noise terms. The variance of noise W can be written as

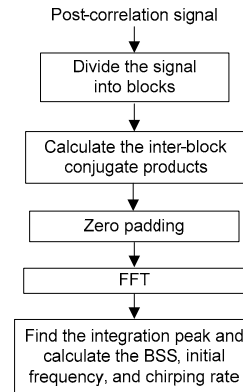


Fig. 1 Block diagram of BASIC

$$\begin{aligned} D(W) &= D\left(w_{kM+i}^* s_{(k+1)M+i} + w_{(k+1)M+i} s_{kM+i}^* \right. \\ &\quad \left. + w_{kM+i}^* w_{(k+1)M+i}\right) \\ &= 2A^2 D(w_n) + D^2(w_n), \end{aligned} \quad (3)$$

where $D(w_n)$ is the variance of w_n . Based on the definition of SNR (Huang *et al.*, 2013), the SNR of inter-block conjugate products is smaller than that of the post-correlation signal:

$$\frac{(A^2)^2}{2A^2 D(w_n) + D^2(w_n)} < \frac{A^2}{D(w_n)}. \quad (4)$$

Based on inequality (4), the process of calculating the inter-block conjugate products reduces the SNR when compared with the initial SNR of the signal.

The DCFT method has been used for L5 signal coherent integration (Fan *et al.*, 2013), and can estimate the initial frequency and chirping rate at the same time. The DCFT of signal x_n can be written as

$$\begin{aligned} y(m, l) &= \sum_{n=0}^{N-1} x_n W_N^{mn + \frac{l}{N} n^2}, \\ 0 \leq m \leq N-1, \quad 0 \leq l \leq N^2-1, \end{aligned} \quad (5)$$

where $W_N = \exp(-j2\pi/N)$. For each fixed l , $\{y(m, l)\}_{0 \leq m \leq N-1}$ is the discrete Fourier transform (DFT) of signal $x_n W_N^{\frac{l}{N} n^2}$. Thus, DCFT can be effectively implemented by FFT and generate N parallel outputs at the same time. The range of l in Eq. (5) seems computationally intensive. In practice, the

computation can be reduced by properly selecting the range of l according to the predicted range of the chirping rate. Additionally, the computation complexity can be further reduced using the fast DCFT algorithm (Aceros-Moreno and Rodriguez, 2005). If $y(m_0, l_0)$ is detected when $m=m_0$ and $l=l_0$, the estimated parameters f_0 and α can be respectively written as

$$f_0 T_s = \frac{m_0}{N}, \tag{6}$$

$$\alpha T_s^2 = \frac{l_0}{N^2}. \tag{7}$$

However, the integration peak is also affected by bit sign. DCFT cannot be directly applied in L1 signal acquisition.

By comparing Figs. 2a and 2b, it can be observed that the post-correlation signal can be coherently integrated by DCFT in the searching zone composed of the initial frequency and chirping rate. Due to the influence of bit sign on the amplitude of integration, the integration peak is hard to detect in Fig. 2a. The

same results can be obtained by comparing Figs. 2c and 2d.

3.2 The proposed method

To estimate parameters in a weak signal and high dynamic environment, we propose the block zero-padding method based on DCFT. At the end of the method, the threshold is set to detect the integration peak. This is proposed to avoid incorrect values of the high dynamic parameters being estimated when the signal is absent or misaligned with the local code. The specific steps of the proposed method can be described as follows (Fig. 3):

Step 1: Divide x_n into several blocks:

$$Y_k^b = [x_{20(k-1)+i+b-1}], \quad i = 1, 2, \dots, M, \tag{8}$$

$$k = 1, 2, \dots, K, \quad b = 1, 2, \dots, M.$$

It is assumed that bit synchronization is obtained when b is equal to b_1 .

Step 2: Write the zero-padding block as

$$h_k = [\mathbf{0}_{M(k-1)} \quad Y_k^{b_1} \quad \mathbf{0}_{N-kM}]. \tag{9}$$

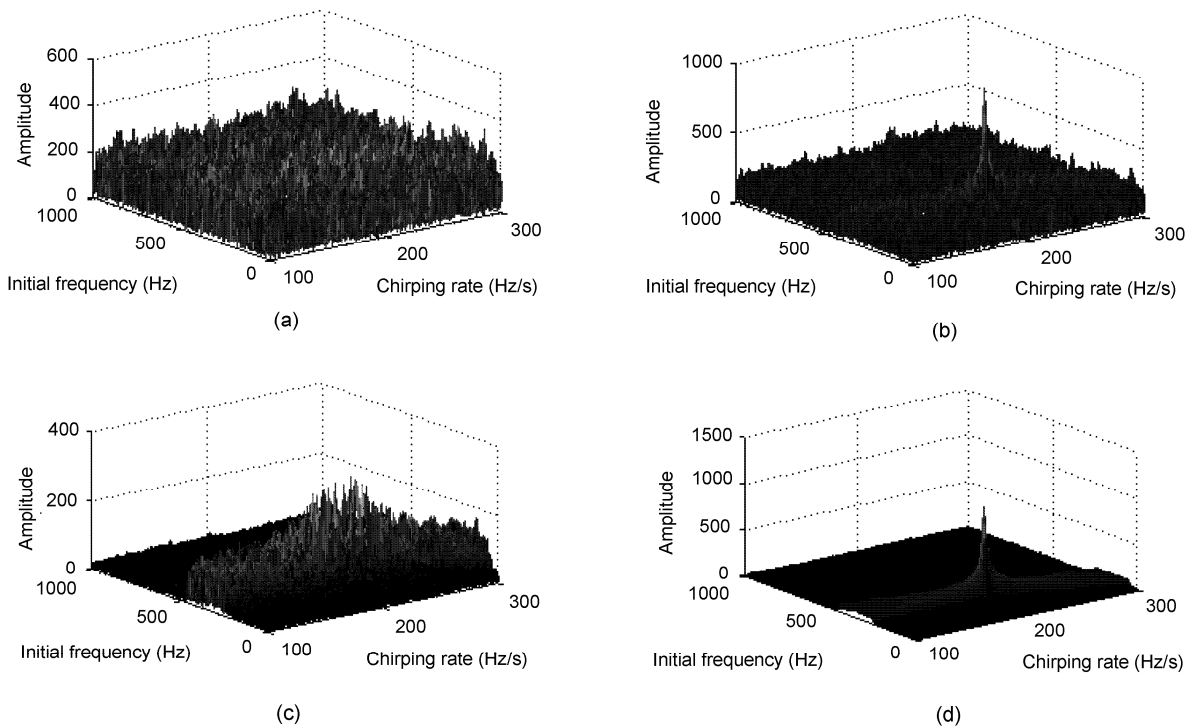


Fig. 2 Amplitude of post-correlation signal after DCFT when the initial frequency is 250 Hz and chirping rate 200 Hz/s (a) -40 dB (SNR), bit sign unknown; (b) -40 dB (SNR), bit sign known; (c) -20 dB (SNR), bit sign unknown; (d) -20 dB (SNR), bit sign known

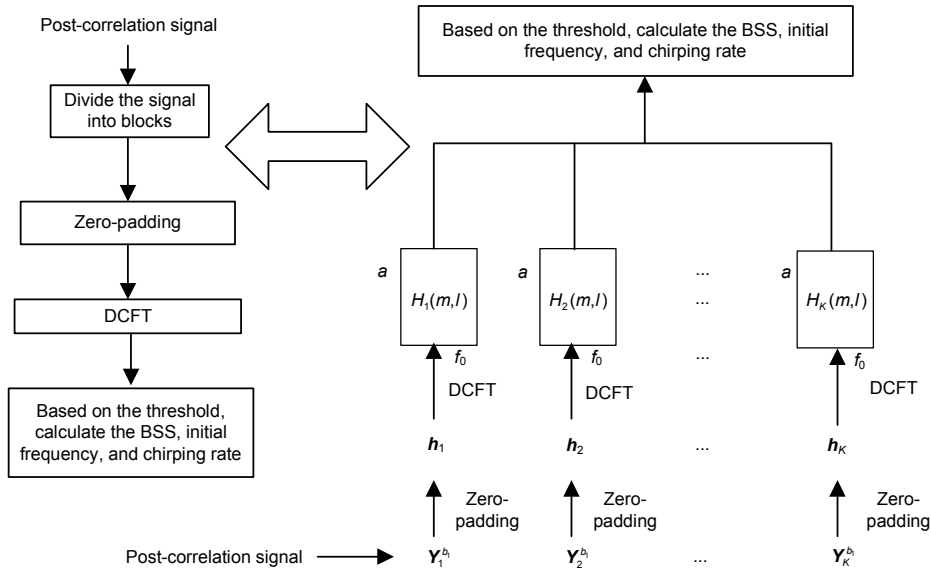


Fig. 3 Diagram of the block zero-padding method based on DCFT

Step 3: Instead of calculating the inter-block conjugate products of x_n (Yang et al., 2008), perform DCFT on h_k :

$$H_k(m, l) = \text{DCFT}(h_k). \tag{10}$$

The k th bit sign can be solved as follows:

$$\delta_k^{b_i}(m, l) = \arg \max_{\delta_k^{b_i}(m, l) \in \{-1, 1\}} \left| S_{k-1}^{b_i}(m, l) + \delta_k^{b_i}(m, l) \cdot \text{real}(H_k^{b_i}(m, l)) \right|, \tag{11}$$

where $\text{real}(\cdot)$ represents the real part. The partial sum $S_k^{b_i}(m, l)$ and bit sign vector $\mathbf{B}_k^{b_i}(m, l)$ can be obtained as follows:

$$S_k^{b_i}(m, l) = S_{k-1}^{b_i}(m, l) + \delta_k^{b_i}(m, l) \text{real}(H_k^{b_i}(m, l)), \tag{12}$$

$$\mathbf{B}_k^{b_i}(m, l) = [\mathbf{B}_{k-1}^{b_i}(m, l) \ \delta_k^{b_i}(m, l)], \tag{13}$$

where $S_0^{b_i}(m, l)$ is equal to 0 and $\mathbf{B}_0^{b_i}(m, l)$ is an empty vector.

Step 4: Make detection based on the set threshold V_i . The threshold is set based on the false alarm probability. If J ($J = |S_K^{b_i}(m_0, l_0)|$) is larger than V_i , the signal is acquired. Thus, the BSS is $\mathbf{B}_K^{b_i}(m_0, l_0)$. Then based on Eqs. (6) and (7), the initial frequency f_0

and chirping rate α can be easily obtained. If not, the local code phase should be updated.

4 Performance analysis of the proposed method

Based on the proposed method, the detection variable J can be written as

$$J = \max_{n_k} \left\{ \left| \sum_{k=1}^K (-1)^{n_k} \text{real}(H_k^{b_i}(m, l)) \right| \right\} = \max \{ |\eta_1|, |\eta_2|, \dots, |\eta_{2^{K-1}}| \}, \tag{14}$$

where $n_k=0$ or 1, $n_1=0$, and $(-1)^{n_k}$ represents the bit sign, $\text{real}(H_k^{b_i}(m, l))$ obeys the normal distribution with mean μ and variance $\sigma_{m,l}^2$, and $\sum_{k=1}^K (-1)^{n_k} \cdot \text{real}(H_k^{b_i}(m, l))$ is the linear combination of $\text{real}(H_k^{b_i}(m, l))$. So, $(\eta_1, \eta_2, \dots, \eta_{2^{K-1}})$ obeys the multi-normal distribution. When the signal is absent or misaligned with the local code, $\mu=0$. Thus, the overall false alarm probability can be written as

$$P_{FA} = 1 - \prod_{m=1}^{M_0} \prod_{l=1}^L (1 - P_{fa,l,m}), \tag{15}$$

where $P_{fa,l,m}$ is the false alarm probability per detected cell. $M_0 \cdot L = N_c$ (N_c is the number of detected cells). $P_{fa,l,m}$ can be written as

$$\begin{aligned}
 P_{fa,l,m} (J \geq \max(\beta_1, \beta_2, \dots, \beta_{2^{K-1}})) \\
 &= 1 - P\{|\eta_1| \leq \beta_1, |\eta_2| \leq \beta_2, \dots, |\eta_{2^{K-1}}| \leq \beta_{2^{K-1}}\} \\
 &\quad \cdot (-1)^{\rho_m^1 + \rho_m^2 + \dots + \rho_m^{2^{K-1}}} \\
 &= 1 - \sum_{m=1}^{2^{K-1}} F\left((-1)^{\rho_m^1} \beta_1, (-1)^{\rho_m^2} \beta_2, \dots, (-1)^{\rho_m^{2^{K-1}}} \beta_{2^{K-1}}\right),
 \end{aligned} \tag{16}$$

where ρ_m^θ is 0 or 1, and $1 \leq \theta \leq 2^{K-1}$. $F(\cdot)$ is the cumulative distribution function (CDF) of the multi-normal distribution with covariance matrix $C_{l,m}$ and mean vector U . $C_{l,m}(\eta_i, \eta_j) = E[(\eta_i - E(\eta_i))(\eta_j - E(\eta_j))]$, and $1 \leq i, j \leq 2^{K-1}$. $\beta_1, \beta_2, \dots, \beta_{2^{K-1}}$ are thresholds. It is assumed that $\beta_1 = \beta_2 = \dots = \beta_{2^{K-1}} = V_t$. When $P_{fa,l,m}$ is set, V_t can be calculated using the numerical solution.

When the signal is aligned with the local code and the estimated parameters (including the chirping rate and initial frequency) are close to the parameters of the received signal, the detected cell can be assumed as (l_0, m_0) , and the detection probability of the proposed method can be written as

$$\begin{aligned}
 P_D (J \geq V_t) \\
 &= 1 - P\{|\eta_1| \leq V_t, |\eta_2| \leq V_t, \dots, |\eta_{2^{K-1}}| \leq V_t\} \\
 &= 1 - \sum_{m=1}^{2^{K-1}} \left[(-1)^{\rho_m^1 + \rho_m^2 + \dots + \rho_m^{2^{K-1}}} \right. \\
 &\quad \left. \cdot F\left((-1)^{\rho_m^1} V_t, (-1)^{\rho_m^2} V_t, \dots, (-1)^{\rho_m^{2^{K-1}}} V_t\right) \right].
 \end{aligned} \tag{17}$$

The mean vector U' can be written as

$$\begin{aligned}
 U'(\eta_m) = \sum_{k=1}^K \left\{ (-1)^{n_k} b_k \right. \\
 \left. \cdot \sum_{n=0}^{M-1} \exp\left[2\pi j\left(\Delta f(n+kM) + \Delta\alpha(n+kM)^2\right)\right] \right\},
 \end{aligned} \tag{18}$$

where $1 \leq m \leq 2^{K-1}$, $\Delta f = f_0 T_s - m_0/N$, and $\Delta\alpha = \alpha T_s^2 - l_0/N^2$.

Fig. 4 shows the detection probabilities under different SNR values. For simplicity, it is assumed that $\Delta f = 0$ and $\Delta\alpha = 0$. It is observed that the theoretical curves almost overlap with the respective actual curves. Since the integration time increases, the de-

tection probability is higher for $K=3$ than for $K=2$ under the same SNR.

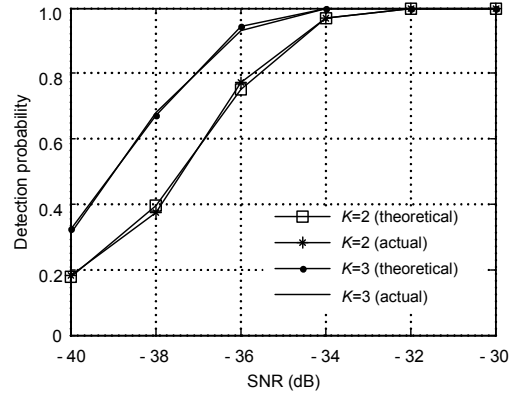


Fig. 4 Detection probabilities under different SNR values using the proposed method ($P_{fa,l,m} = 2 \times 10^{-4}$, $f_0 = 100$ Hz, $\alpha = 200$ Hz/s)

5 Simulation results

The following simulation is conducted to verify that compared with BASIC, the proposed method can acquire the high dynamic parameters (including BSS, chirping rate, and initial frequency) of the L1 signal in a lower SNR. It is assumed that the range of the chirping rate is [100, 300] Hz/s, and the range of the initial frequency is [0, 250] Hz. The parameter settings are listed in Table 1.

Figs. 5a and 5b illustrate the amplitude of $\text{real}(S_K^h(m, l))$ when SNR is equal to -40 and -20 dB, respectively. Figs. 6a and 6c show the amplitude of $\text{real}(S_K^h(m, l))$ when $m = m_0$ under -40 and -20 dB, respectively. Figs. 6b and 6d show the results of using BASIC to estimate the chirping rate under different SNR values.

As Fig. 1 shows, BASIC performs the FFT on the inter-block conjugate products through the zero-padding process, and detects the integration peak to estimate the chirping rate. Figs. 6b and 6d show the amplitude of integration through the FFT process as a function of the chirping rate. As can be seen in Fig. 6d, there is a peak when the chirping rate is 200 Hz/s. However, when SNR is -40 dB, the peak cannot be seen. This is because the process of calculating the inter-block conjugate products brings more noise than

that of the post-correlation signal. So, the integration peak is embedded in noise. As shown in Figs. 6a and 6c, the integration peak can be seen under both -40 and -20 dB. It proves that compared with BASIC, the proposed method can precisely acquire the chirping rate under a relatively low SNR.

To further demonstrate that the proposed method performs better than BASIC under the low SNR scenario, we use Monte Carlo simulation to test their performances in estimating the chirping rate. Fig. 7 presents the detection probability as a function of SNR.

Table 1 Simulation parameters

Parameter	Value
Initial frequency, f_0	100 Hz
Chirping rate, α	200 Hz/s
Number of blocks, K	50
Sampling interval, T_s	1 ms
Number of sampling points per block, M	20
Parameter of DCFT, N	1000
False alarm probability per detection cell	2×10^{-4}
Number of Monte Carlo simulations	10^4

As shown in Fig. 7, the detection probabilities of BASIC and the proposed method both increase with the improvement of SNR. The probability of the proposed method is higher than that of BASIC under

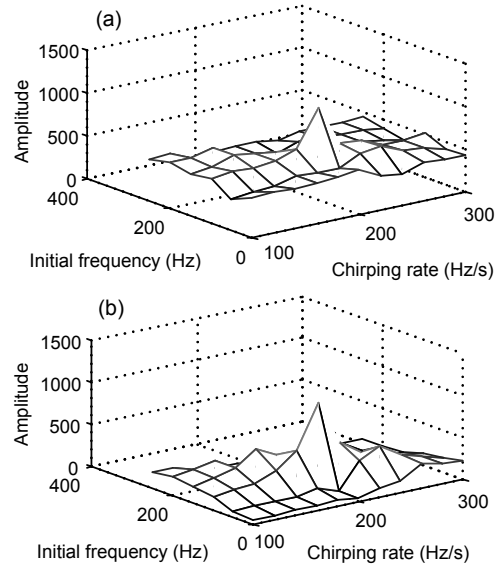


Fig. 5 Amplitude of the partial sums under -40 dB (a) and -20 dB (b)

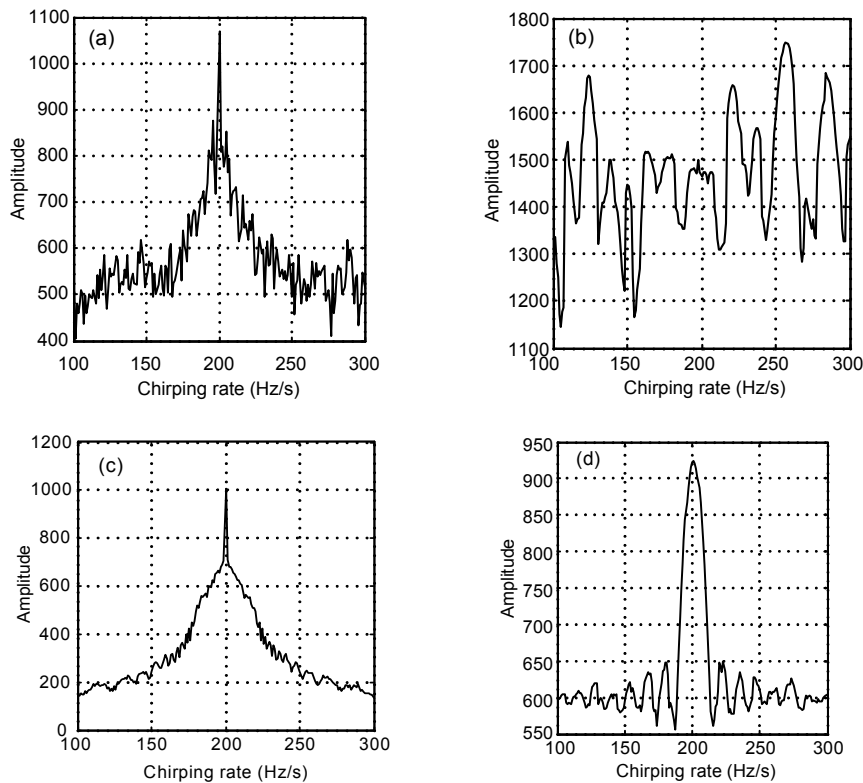


Fig. 6 Chirping rate comparison

(a) Proposed method under -40 dB; (b) BASIC under -40 dB; (c) Proposed method under -20 dB; (d) BASIC under -20 dB

the same SNR. When SNR is equal to -40 dB, the probability of the proposed method is approximately 1, while the probability of BASIC is approximately 0.

Tables 2 and 3 show the BSS obtained by the proposed method and BASIC under -20 and -40 dB, respectively. As can be seen in Table 2, the BSS obtained by the proposed method and b_k^p are the same as the original sequence. It proves that both the proposed method and BASIC can obtain the true value of the bit sign. However, as shown in Table 3, under the lower SNR value (-40 dB), some error bit signs occur in the BSS obtained by BASIC. In contrast, the BSS obtained by the proposed method is still the same as

the original BSS. This further proves that the proposed method outperforms BASIC in deriving a correct bit sign in a lower SNR circumstance.

6 Conclusions

This paper combines the BASIC method and DCFT method, and proposes the block zero-padding method based on DCFT for parameter estimation in a weak signal and high dynamic environment. First, the high dynamic post-correlation signal model is presented. Then this paper analyzes the process of calculating the inter-block conjugate products of BASIC, which reduces the SNR compared with the initial SNR of the signal. The fact that DCFT cannot be directly used in the L1 acquisition under the low SNR has been presented. Based on the analysis, the block zero-padding method based on DCFT is proposed. In this way, the post-correlation signal is coherently post-integrated, and the influence of BSS on the integration peak is eliminated. The high dynamic parameters can be estimated based on the set threshold. Finally, the performance of the proposed method is analyzed. The simulation shows that compared with BASIC, the proposed method can estimate the high

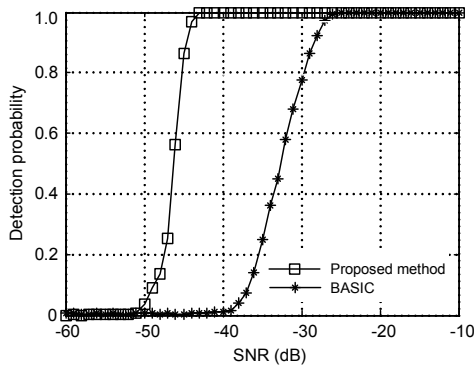


Fig. 7 Detection probability comparison between the proposed method and BASIC

Table 2 Bit sign sequence (BSS) determination (SNR=-20 dB)

Item	Bit sign																			
	k=1	2	3	4	5	6	7	8	9	10	11	12	13	14	15	16	17	18	19	20
Original	1	1	-1	1	1	-1	-1	1	1	1	-1	1	1	-1	1	-1	-1	1	1	1
Proposed method	1	1	-1	1	1	-1	-1	1	1	1	-1	1	1	-1	1	-1	-1	1	1	1
BASIC																				
δ_k	-	1	-1	-1	1	-1	1	-1	1	1	-1	-1	1	-1	-1	-1	1	-1	1	1
b_k^p	1	1	-1	1	1	-1	-1	1	1	1	-1	1	1	-1	1	-1	-1	1	1	1
b_k^n	-1	-1	1	-1	-1	1	1	-1	-1	-1	1	-1	-1	1	-1	1	1	-1	-1	-1

Table 3 Bit sign sequence (BSS) determination (SNR=-40 dB)

Item	Bit sign																			
	k=1	2	3	4	5	6	7	8	9	10	11	12	13	14	15	16	17	18	19	20
Original	1	1	-1	1	1	-1	-1	1	1	1	-1	1	1	-1	1	-1	-1	1	1	1
Proposed method	1	1	-1	1	1	-1	-1	1	1	1	-1	1	1	-1	1	-1	-1	1	1	1
BASIC																				
δ_k	-	1	1	1	-1	1	1	1	-1	-1	1	-1	-1	-1	-1	-1	1	1	1	-1
b_k^p	1	1	1	1	-1	-1	-1	-1	1	-1	-1	1	-1	1	-1	1	1	1	1	-1
b_k^n	-1	-1	-1	-1	1	1	1	1	-1	1	1	-1	1	-1	1	-1	-1	-1	-1	-1

dynamic parameters under a lower SNR. In contrast to the conventional receiver architecture using the closed-loop acquisition and tracking method, this is an open-loop acquisition method. It is particularly suitable for software radio receivers with snapshot solutions.

References

- Aceros-Moreno, C.A., Rodriguez, D., 2005. Fast discrete chirp Fourier transforms for radar signal detection systems using cluster computer implementations. Proc. 48th Midwest Symp. on Circuits and Systems, p.1047-1050. [doi:10.1109/MWSCAS.2005.1594284]
- Belega, D., Dallet, D., 2008. Frequency estimation via weighted multipoint interpolated DFT. *IET Sci. Meas. Technol.*, **2**(1):1-8. [doi:10.1049/iet-smt:20070022]
- Dai, L., Wang, Z., Wang, J., et al., 2010. Joint code acquisition and Doppler frequency shift estimation for GPS signals. Proc. IEEE 72nd Vehicular Technology Conf., p.1-5. [doi:10.1109/VETECF.2010.5594093]
- Fan, B., Zhang, K., Qin, Y., et al., 2013. Discrete chirp-Fourier transform-based acquisition algorithm for weak Global Positioning System L5 signals in high dynamic environments. *IET Radar Sonar Navig.*, **7**(7):736-746. [doi:10.1049/iet-rsn.2012.0249]
- Fu, H., Kam, P.Y., 2007. MAP/ML estimation of the frequency and phase of a single sinusoid in noise. *IEEE Trans. Signal Process.*, **55**(3):834-845. [doi:10.1109/TSP.2006.888055]
- Geiger, B.C., Vogel, C., 2013. Influence of Doppler bin width on GPS acquisition probabilities. *IEEE Trans. Aerosp. Electron. Syst.*, **49**(4):2570-2584. [doi:10.1109/TAES.2013.6621837]
- Geiger, B.C., Vogel, C., Soudan, M., 2012. Comparison between ratio detection and threshold comparison for GNSS acquisition. *IEEE Trans. Aerosp. Electron. Syst.*, **48**(2): 1772-1779. [doi:10.1109/TAES.2012.6178098]
- Huang, P., Pi, Y., Progni, I., 2013. GPS signal detection under multiplicative and additive noise. *J. Navig.*, **66**(4): 479-500. [doi:10.1017/S0373463312000550]
- Kay, S., 1989. A fast and accurate single frequency estimator. *IEEE Trans. Acoust. Speech Signal Process.*, **37**(12): 1987-1990. [doi:10.1109/29.45547]
- Li, X., Guo, W., 2013. Efficient differential coherent accumulation algorithm for weak GPS signal bit synchronization. *IEEE Commun. Lett.*, **17**(5):936-939. [doi:10.1109/LCOMM.2013.031913.130267]
- Li, X., Guo, W., Xie, X., 2011. A GPS bit synchronization method for high-dynamic and weak signal. *J. Electron. Inform. Technol.*, **33**(10):2521-2525 (in Chinese). [doi:10.3724/SP.J.1146.2011.00270]
- Shanmugam, S.K., Nielsen, J., Lachapelle, G., 2007. Enhanced differential detection scheme for weak GPS signal acquisition. Proc. Int. Technical Meeting of the Satellite Division of the Institute of Navigation, p.1-14.
- Spangenberg, S.M., Scott, I., McLaughlin, S., et al., 2000. An FFT-based approach for fast acquisition in spread spectrum communication systems. *Wirel. Pers. Commun.*, **13**(1-2):27-55. [doi:10.1023/A:1008848916834]
- Su, Y.T., Wu, R.C., 2000. Frequency acquisition and tracking in high dynamic environments. *IEEE Trans. Veh. Technol.*, **49**(6):2419-2429. [doi:10.1109/25.901910]
- Yang, C., Han, S., 2001. Block-accumulating coherent integration over extended interval (BACIX) for weak GPS signal acquisition. Proc. 19th Int. Technical Meeting of the Satellite Division of the Institute of Navigation, p.2427-2440.
- Yang, C., Nguyen, T., Blasch, E., et al., 2008. Post-correlation semi-coherent integration for high-dynamic and weak GPS signal acquisition. Proc. IEEE/ION Position, Location and Navigation Symp., p.1341-1349. [doi:10.1109/PLANS.2008.4570122]